Data-driven Model Predictive Control for Drop Foot Correction

Mayank Singh, Nitin Sharma*

Functional Electrical Stimulation (FES) is an effective method to restore the normal range of ankle motion in people with Drop Foot. This paper aims to develop a real-time, data-driven Model Predictive Control (MPC) scheme of FES for drop foot correction (DFC). We utilize a Koopman operator-based framework for system identification required for setting up the MPC scheme. Using the Koopman operator we can fully capture the nonlinear dynamics through an infinite dimensional linear operator describing the evolution of functions of state space. We use inertial measurement units (IMUs) for collecting the foot pitch and roll rate state information to build an approximate linear predictor for FES actuated ankle motion. In doing so, we also account for the implicit muscle actuation dynamics which are dependent on the activation and fatigue levels of the Tibialis Anterior (TA) muscle contribution during ankle motion, and hence, develop a relationship between FES input parameters and ankle motion, tailored to an individual user. The approximation, although computationally expensive, leads to reformulating the optimization problem as a quadratic program for the MPC problem. Further, we show the closed-loop system's recursive feasibility and asymptotic stability analysis. Simulation and experimental results from a subject with Multiple Sclerosis show the effectiveness of the data-driven MPC scheme of FES for DFC.

I. INTRODUCTION

Persons with drop foot, common in those with neurological impairments due to stroke, spinal cord injury, and multiple sclerosis, can benefit from advanced functional electrical stimulation (FES)-based gait assistance systems. Numerous challenges hinder the effectiveness of current FES systems for drop foot correction (DFC). Experiments demonstrate that the degree of foot lift induced by FES at a given intensity is highly subject-dependent, varies with time, and is sensitive to modest (~1 cm) changes in electrode position [1]. The stimulation parameters need reconfiguration every time the gait assistance system is utilized, to produce a physiological foot lift in the paretic limb. Although many complex models

M. Singh is with the Department of Electrical Engineering, North Carolina State University-Raleigh. (Email: msingh25@ncsu.edu). Nitin Sharma is with the UNC/NC State Joint Department of Biomedical Engineering, NC State University -Raleigh, NC 27606 USA (e-mail: nsharm23@ncsu.edu).

*Corresponding author: Nitin Sharma. This work was funded by NSF Award #2002261 and by NSF Award #2124017.

have been used to represent dynamic muscle responses to FES, there is no consensus on the most optimal model in the literature. Moreover as the FES actuation dynamics implicitly affect limb motion, the control synthesis problem is extremely challenging. To address these challenges, we develop a novel data-driven control scheme that does not use system identification methods for estimating subject-dependent parameters for optimal closed-loop control synthesis.

FES has been utilized in several different implementation settings to correct drop foot. A comprehensive survey can be found in [2]. [3] used an adaptive torque tracking method for DFC, wherein sEMG based activation signals were designed, and the model identification was performed through Kalman filtering techniques. [4] used a MPC framework for offline trajectory optimization. While constraints on ankle and control inputs were considered, a formal closed-loop stability and control feasibility analysis were missing. In [5], [6] FES MPC controller was proposed and was later extended to robust MPC schemes in [7] and [8] for knee regulation and tracking, respectively. While MPC framework yields optimal inputs for FES, which are useful in avoiding overstimulation and are constrained within prescribed stimulation intensity limits, the aforementioned MPC schemes require extensive system identification of the nonlinear musculoskeletal system. In this regard, a data-driven approach is much more attractive than traditional modeling approaches for MPC-based control of

To analyze the nonlinear dynamics of the ankle under FES actuation, and motivated to derive a data-driven approach, we utilize a Koopman framework to predict the dynamics and subsequently design an MPC scheme. The Koopman operator is an infinite-dimensional linear operator which captures the nonlinear dynamical characteristics through a linear dynamic evolution on a lifted observable function of states [9]. Recent work in [10], [11] has shown the effectiveness of the Koopman operator framework to analyze non-autonomous dynamical systems for optimal control synthesis. In [11], a finite-dimensional truncation of the Koopman operator was used to form a linear predictor of nonlinear dynamics for designing a linear MPC. MPC methods utilizing a deep learning-based Koopman model were developed in [12].

We develop a data-driven Koopman observable-based ankle joint model to facilitate FES-based ankle joint torque modulation and further develop an MPC scheme with results on recursive feasibility and asymptotic stability of the datadriven closed-loop system. The novelty of the work is that the system and the optimal control is designed for a cascaded non-affine system in the control input without prior system identification methods. We tested the developed control scheme in simulations and experiments, wherein a subject with Multiple Sclerosis used the developed FES-based DFC controller.

The paper is organized as follows – Section II describes the ankle dorsiflexion motion dynamics actuated under FES. Section III discusses the overview of the Koopman-based system identification for ankle dynamics and the subsequent formulation of the MPC-based control synthesis problem. Both feasibility and asymptotic stability results are derived in Section III. Data collection, experimental setup, simulation, and experiment results are discussed in IV. Finally, the paper concludes in Section V with some discussion on future work.

II. ANKLE JOINT DORSIFLEXION MOTION DYNAMICS

A multi-dimensional dynamic model of the FES-actuated ankle movement

$$J\ddot{\theta} + M_q(\theta, \theta_{eq}) + M_v(\dot{\theta}) + M_e(\theta) + d(t) = \tau, \quad (1)$$

where $J \in \mathbb{R}^{2 \times 2}$ is the unknown inertia matrix of the foot along the dorsiflexion/plantarflexion and inversion/eversion axis of rotation, $\theta, \dot{\theta}, \ddot{\theta} \in \mathbb{R}^2$ denote the pitch and roll angle, pitch and roll rate, and pitch and roll acceleration, respectively. $M_g(\theta, \theta_{eq}), M_v(\dot{\theta}),$ and $M_e(\theta) \in \mathbb{R}^2$ represent the gravitational, passive moment, and musculoskeletal elasticity vector. The constant limb equilibrium point is represented as θ_{eq} , which represents the joint is at a posture when the limb is completely relaxed. The gravitational term is described as $M_g(\theta, \theta_{eq}) = mglsin(\frac{\pi}{2} + \theta + \theta_{eq})$. The mass of the limb and the length from the limb's center of mass to its rotation center in the sagittal plane are denoted as $m \in \mathbb{R}^+$ and $l \in \mathbb{R}^+$, respectively. The explicit definitions of the functions, $M_v(\dot{\theta})$ and $M_e(\theta)$, can be obtained from [6], [13]. The term related to external disturbance is denoted as $d(t) \in \mathbb{R}^2$.

The net torque about the ankle is defined as $\tau = \rho(\theta,\dot{\theta})\phi u$, where $\rho(\theta,\dot{\theta}) \in \mathbb{R}^{2 \times 2}$ represents the force-length, force-velocity term, $\phi \in \mathbb{R}^2$ represents the muscle fatigue term, and $u \in \mathbb{R}$ is the FES modulated parameter (current, pulse width, or frequency) applied on the TA muscle. The expression for terms $\rho(\theta,\dot{\theta})$, ϕ can be found in [6].

By selecting $\theta_1 = \theta$ and $\theta_2 = \theta$, the equivalent state space representation for (1) can be formulated as

$$\dot{x}_a = f(x_a) + g(x_a, u)u,\tag{2}$$

where $\dot{x}_a = \begin{bmatrix} \dot{\theta}_1 & \dot{\theta}_2 \end{bmatrix}^T$, $f(x_a) \in \mathbb{R}^4$ are the system dynamics, and $g(x_a,u) \in \mathbb{R}^4$ are the actuation dynamics.

Assumption 1: The inertia term, J, is positive and bounded as $J_l \leq ||J|| \leq J_u$, where J_l , $J_u \in \mathbb{R}^+$.

Assumption 2: The disturbance term, d(t), is bounded as $||d(t)|| \le d_u$, where d_u is a positive constant.

We can now set up the optimal tracking problem by defining a tracking error $e(t) \in \mathbb{R}^4$ is defined as

$$e = x_a - x_d, (3)$$

where $x_d \in \mathbb{R}^2$ is a bounded desired trajectory for the desired position and velocity. It is assumed that x_d and its first derivative, $\dot{x}_d = h_d(x_d) \in \mathbb{R}^2$, are Lipschitz continuous.

Taking the derivative of (3) gives the error dynamics

$$\dot{e}(t) = \dot{x}_a - \dot{x}_d
= f(x_a) + g(x_a, u)u - h_d(x_d),$$
(4)

By defining an augmented state as $x = \begin{bmatrix} e^T & x_d^T \end{bmatrix}^T \in \mathbb{R}^6$ the system dynamics can be written as

$$\dot{x} = f(x) + g(x, u)u,\tag{5}$$

where the system matrices f(x) and g(x, u) matrices become

$$f(x) = \begin{bmatrix} f(e+x_d) - h_d(x_d) \\ h_d(x_d) \end{bmatrix}; g(x,u) = \begin{bmatrix} g(e+x_d) \\ 0 \end{bmatrix}.$$

Using zero order hold approximation the continuous-time system in (5) can be discretized and described as

$$x_{k+1} = f_e(x_k) + g_e(x_k, u_k)u_k \tag{6}$$

III. KOOPMAN-BASED MODEL PREDICTIVE CONTROL

A. Prediction/Identification

The Koopman operator κ is an infinite-dimensional linear operator that models the time-based evolution of a composite function $\Lambda(x_k) \in \mathbb{R}^{\infty}$, known as the *koopman observables*, forward in time. The function, $\Lambda(x_k)$, can be the state themselves or nonlinear functions of state that are Lipschitz continuous. Appropriate choice for synthesis of such basis functions can be found in [14]. This framework provides an accurate linear representation of the original complex nonlinear dynamics without any loss of accuracy [15], but increases the dimensionality of the original system. The idea can be extended to non-autonomous systems as well, see [9]. Mathematically, this can be represented as

$$\Lambda(x_{k+1}) = \kappa \Lambda(x_k) \tag{7}$$

While this operator renders an infinite-dimensional system and accurately describes a nonlinear system through a linear system, but is practically infeasible to implement. For practical feasibility, the infinite-dimensional operator, κ , is approximated using a finite dimensional operator, $\tilde{\kappa}$, which can be found by setting up a dynamic regression problem of analyzing the evolution finite-dimensional Koopman observable vector, $\Lambda(x_k, u_k) \in \mathbb{R}^P$, which for non-autonomous systems is a function of control inputs as well.

To obtain the approximate Koopman operator for DFC, we first collect M time snapshots of the state and control data vectors as

$$X_k = [x_1 \dots x_M]; \quad U_k = [u_1 \dots u_M]$$
 (8)

where X_k and U_k represent the prediction dynamics state vector. The state and control vectors are further used to populate the Koopman observable vector, $\Lambda_k(x,u) \in \mathbb{R}^p$, given as

$$\Lambda_k(x, u) = \begin{bmatrix} x_k^T & u_k^T & \Lambda_1(.)^T & \dots & \Lambda_W(.)^T \end{bmatrix}^T, \quad (9)$$

 $\forall k=1,\ldots,m,$ with the collected data snapshots from FES inputs and /IMU measurements (outputs). The selection of basis functions, $\Lambda(.)$, in (9) has been inspired from [12]. The Koopman observable vector dynamically evolves as

$$\Lambda_{k+1}(x,u) = \tilde{\kappa}\Lambda_k(x,u), \tag{10}$$

where $\tilde{\kappa} \in \mathbb{R}^{P \times P}$. It is important to note that the first n+m columns of $\tilde{\kappa}$ govern the state and control vector evolution between the k^{th} and the $k+1^{th}$ instants. To obtain $\tilde{\kappa}$, a dynamic regression problem is set up and solved using least-squares methods to the calculate the approximate Koopman operator.

The minimization problem can be set up as

$$\tilde{\kappa}^* = arg \min_{\tilde{\kappa}} \sum_{k=0}^{M-1} 0.5 ||\Lambda_{k+1}(x, u) - \tilde{\kappa} \Lambda_k(x, u)||^2,$$
 (11)

where $\tilde{\kappa}$ can be obtained by calculating the gradient of the minimization function in (11) with respect to $\tilde{\kappa}$, and equating the resultant to zero. We obtain the approximate Koopman operator as $\tilde{\kappa}=FG^{\dagger}$, where

$$F = \frac{1}{M} \sum_{k=0}^{M-1} \Lambda_{k+1}(x, u) \Lambda_k(x, u)^T$$

$$G = \frac{1}{M} \sum_{k=0}^{M-1} \Lambda_k(x, u) \Lambda_k(x, u)^T.$$
(12)

We can subdivide the Koopman operator as $\tilde{\kappa} = \left[\tilde{\kappa}_x \quad \tilde{\kappa}_u\right]$, where the submatrix $\tilde{\kappa}_x \in \mathbb{R}^{n \times P}$ denotes the propagation of state-dependent Koopman observables, $\Lambda_k(x) \in \mathbb{R}^n$, and $\tilde{\kappa}_u \in \mathbb{R}^{m \times P}$ denotes the propagation of control-dependent Koopman observables, $\Lambda_k(u) = u_k \in \mathbb{R}$, where 1 + n = P. Now, to obtain the Koopman prediction dynamics for FES-driven DFC described in for (6), we can redefine (10) in terms of the evolution of the state-dependent Koopman observable governed by $\tilde{\kappa}_x$, $\tilde{\kappa}_u$ as

$$\Lambda_{k+1}(x) = \tilde{\kappa}_x \Lambda_k(x) + \tilde{\kappa}_u u_k = f_{\kappa}(\Lambda_k, u_k). \tag{13}$$

This results is a linear prediction dynamics for FES-driven DFC in the state dependent observable $\Lambda_k(x)$. To obtain the prediction dynamics for the original state in (5), we compute the flow map between $\Lambda_k(x,u)$ and x, we setup another least square minimization problem similar in (11). We redefine the state vector x_k as z_k to avoid any notational confusion with (II). To recover z_k , we can describe the mapping between Koopman observable, $\Lambda_k(x)$, and z_k as $z_k = C\Lambda_k(x)$, where $C \in \mathbb{R}^{6 \times P}$ denotes the mapping. To obtain C, we can setup another minimization problem as

$$arg \min_{C} \sum_{k=0}^{M-1} \frac{1}{2} ||C\Lambda_k(x, u) - z_k||^2.$$
 (14)

By solving (14), and plugging $\Lambda_k(x, u) = C^{-1}z_k$ in (13), we obtain the linear prediction dynamics for FES-driven DFC as

$$z_{k+1} = A(z_k)z_k + B(z_k)u_k (15)$$

B. Data-driven model predictive control

Let the decision and state variables be defined as

$$u_k = [u_{k|k} \dots u_{k+N-1|k}],$$
 (17)

where the vectors $z_k, u_k \in \mathbb{R}^6$, \mathbb{R} are the state and control vectors written in the standard MPC notation. MPC prediction dynamics can be defined as $z_{k+1+i|k} = A(z_k)z_{k+i|k} + B(z_k)u_{k+i|k}$.

The model predictive problem can then be formulated as follows

$$\min_{u_{k|k}} J(z_k, u_{k|k}) = \sum_{i=1}^{T_U - 1} l(.) + V(z_{k+T_U})$$
 (18)

subject to

$$z_{k+1+i|k} = A(z_k)z_{k+i|k} + B(z_k)u_{k+i|k}$$
 (a)

$$z_{k|k} \in \Omega_{\chi}, \ u_{k|k} \in \Omega_{v} \tag{b}$$

$$\Delta z_{k+T_N} \in \Omega_{\chi^+},\tag{c}$$

where $V(z_{k+T_U|k}) = z_{k+T_U}^T P z_{k+T_U}$ is the terminal cost. T_N and T_U are the prediction and control horizon, respectively. The running cost is $l(.) = z_{k+i+1|k}^T Q z_{k+i+1|k} +$ $u_{k+i|k}^T R u_{k+i|k}$ is the performance measure penalizing the kinematic state and control inputs considered over the control horizon, T_U . $Q \in \mathbb{R}^{n \times n}$ and $R \in \mathbb{R}^{m \times m}$ are positive definite weighting matrices penalizing the individual states and control inputs and ensures l and V are positive definite (PD) and radially unbounded (RU). The control input u has asymmetric saturation bounds captured in the control set $\Omega_v \in \mathbb{R}$, and $\mathbb{X} \in \mathbb{R}^p$ is the set of allowable states. Ω_v denotes the actuator's limits and Ω_{χ} denotes the set of the state constraints. (As the current time step is fixed based on the number of samples, z_k will be used instead of $z_{k|k}$, and system matrices derived over M samples will be denoted by A, B to reduce notational burden).

The desired input vector u_k is computed from the nominal model to achieve a given desired state x_d . Thus, the pair (x_d, u_k) is the equilibrium point of the system.

Defining the optimal control input trajectory as $\bar{u}_k^* = \bar{u}^*$. The first control input $\bar{u}^*(k|k:k\to k+1)$, is applied for an interval defined as $\Delta k = 1$. The corresponding optimal state sequence is defined as $z^*(k|k:k\to k+1)$. The terminal region, Ω_{χ^+} is the terminal set constraint.

Assumption 5: In (18) the function V, l, are continuous, f_{κ} is twice continuously differentiable, $u_k \mapsto l(z_k, u_k)$ is coercive, and V(0) = 0, l(0,0) = 0, f(0,0) = 0. The set Ω_v is compact, uniformly bounded and contains the origin.

Assumption 6: There exist \mathcal{K}_{∞} functions α_l and α_V , so that $\alpha_l(||z||) \leq l(z_k, u_k)$, $\alpha_V(||z||) \leq V(z_N)$.

Assumption 7: There exist an optimal input trajectory $\bar{u}_{k+1|k}^*$ for and a non-empty feasible region around $(z_{initial}^*, u_{initial}^*)$.

By choosing appropriate lifting functions, the Koopmandriven dynamics in (13) and (15) are controllable. A controller gain K_f for the terminal controller $u_k^* = K_f z_k$ such that $A + BK_f$ is asymptotically stable is determined.



Figure 1. Seated task setup - The electrodes were placed on the TA muscle with stimulation parameters set at $f=50 {\rm Hz},~i=25 {\rm mA},$ and the pulse width was varied to determine the threshold and saturation values for ankle dorsiflexion and use them further for system identification, and the inertial measurement unit was placed on the shank and the foot.

Choose a constant $\eta \in \mathbb{R}^+$ satisfying the inequality $\eta < -\lambda_{max}(A+BK_f)$ and solve the following Lyapunov equation to determine a positive-definite and symmetric P

$$(A + BK_f + \eta I)^T P + P(A + BK_f + \eta I)$$

 $+ Q + K_f^T RK_f \le 0.$ (19)

Then, using Lemma 1 in [16], one can show that

$$V(z_{k+1}) - V(z_k) + l \le 0 (20)$$

which implies that $u_k^* = K_f z_k$ is invariant in Ω_v and satisfies the input constraints.

Assuming \bar{u}_k^* exists for $k \in [k, k+1]$, the next feasible solution for $t \in [k+1, k+1+T_u]$ is constructed as

$$\hat{u}_{k+1|k} = \begin{cases} \bar{u}_k^*, & k \in [k+1 \, k + T_U) \\ \kappa_N(z_{k+1}), & t \in [k+T_U, \, k+1 + T_U) \end{cases}$$
(21)

where $K_{f+1}(z_{k+1}) = u_k^* - K_f z_{k+1}$.

Theorem 1. The MPC algorithm is (i) recursively feasible and (ii) asymptotically stable by defining the actual optimal control sequence u_k^* , if $u_{k+1|k}^*$ exists for $\forall k \in [1, T_U]$.

Proof: Theorem 1 proof is available upon request.

IV. SIMULATION & EXPERIMENTAL RESULTS

A. Data Collection & Experiments

The study was approved by the IRB at North Carolina State University (IRB number: 20602).

Participants: Four able-bodied subjects (A07, A08,A09, A10, 4M, age: 27.4 \pm 3.1 years, height: 1.73 \pm 0.15 m, mass: 82.0 \pm 7.1 kg) without any neuromuscular or orthopedic disorders were recruited.

Seated task: Fig. (1) illustrates the data-collection experimental setup for repetitive seated position experiments. Each participant was seated on a level seat table with adjustable height, and the right foot was kept suspended in the air by adjusting the chair height. The initial right ankle equilibrium position ($\theta=0^{\circ}$) for each experimental trial was set at the position where the participants felt completely relaxed

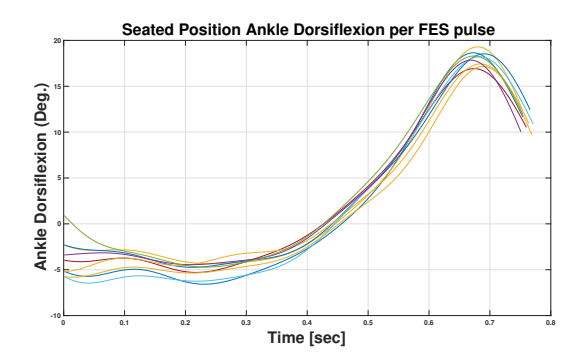


Figure 2. Ankle dorsiflexion response (threshold-saturation) for a constant frequency (55Hz), current amplitude (30mA), and varying pulse width duration [$100 \, \mu s - 350 \, \mu s$]. The figure shows the dorsiflexion response of 5 subjects (4 able bodied).

about their right shank and foot. The threshold and saturation levels for stimulation pulse width were determined using the isometric dorsiflexion experiment based on [6] For IMU and FES input data collection for ankle dorsiflexion, we placed the FES electrodes on the fibular head and the lateral malleolus of the TA muscle. The stimulation current and frequency were kept constant, while the pulse-width was chosen as the modulation parameter. Three trials per subject were conducted with varying pulse width values to collect the FES and ankle motion data. A 3-minute rest time was provided for the participant to avoid TA muscle fatigue. The collected average ankle dorsiflexion movement under one trapezoidal pulse is presented in Fig.(2).

Data collection: Based on [17], a wearable sensing system was used to measure the ankle joint kinematics. Along with measuring the ankle kinematics, IMU measurements were also used for gait phase detection based on methods discussed in [18], [19]. Details on obtaining ankle angle from IMU measurements can be found in [20]. The ankle pitch and roll, and FES input signals were collected as (8) to derive the Koopman prediction dynamics described in (13). Utilization of the collected data is shown in subsequent section.

B. Prediction & Simulation Results

Simulation were performed by using the parameters from [6] with different initial conditions to obtain the samples of actual system trajectories. For Koopman prediction dynamics synthesis, we use M(=300) sample ankle pitch and roll trajectories for different stimulation and subject parameters The measured samples consisted both simulations and subject data (described in (IV-A)). To generate a lifted system we considered different basis function for Koopman observables - radial basis functions and polynomial based on [14], and compared their prediction accuracies. Polynomial basis function gave prediction accuracy of 93.7% per swing phase as shown in Fig. (3). The Koopman observables was defined as $\Lambda_k(x,u) = \begin{bmatrix} x & \Lambda_k^1(x) & \dots & \Lambda_k^W(x) & \Lambda_k(u) \end{bmatrix}$, where $\Lambda_k^i(x) = e^a + x_d^b \ \forall i = 1,\dots,W, \ a,b \in \mathbb{R}^+$, and $\Lambda_k(u) = u \in \mathbb{R}$ where e, x_d are the error and reference trajectories described in (5). Based on the prediction dynamics,

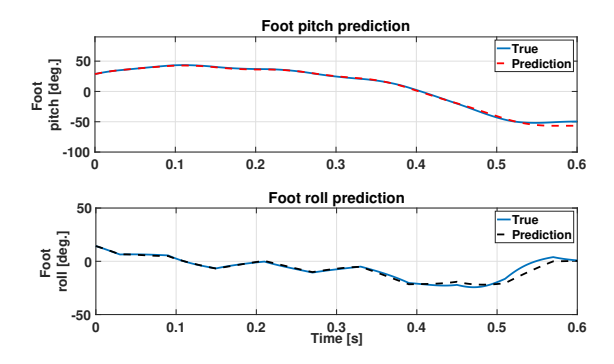


Figure 3. *Prediction results* - Plot shows the foot pitch and foot roll prediction dynamics under test FES actuation. The dynamics approximated from (13) are utilized to predict the approximate dynamics.

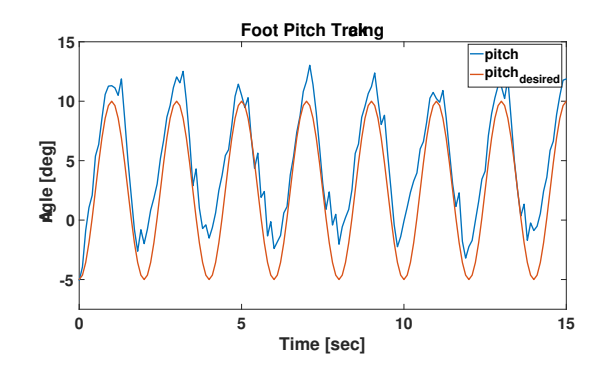


Figure 4. Simulation results - The plot shows the tracking response of foot pitch with respect to a desired sinusoidal trajectory.

simulation results for a nominal sinusoidal trajectory tracking of the ankle pitch are given in Fig. (4).

C. Experiments & Results

Participants: One subject with Multiple Sclerosis (MS) (S01, age: 67 years, height: 156 m, weight: 57 kg) participated in the study.

 $Walking\ task$: The walking tasks were set up as level ground walking to complete 8 steps with the FES actuation provided on the TA muscle during the swing phase. The walking setup is illustrated in Fig. (5). The FES electrodes were placed on the fibular head and the lateral malleolus of the TA muscle. The FES inputs were designed using the data-driven methods described in (18) and (21), and implemented with IMU-based gait phase detection. The primary objective of these task was to avoid any foot drag and achieve adequate foot clearance (pitch, $x_1 > 12deg$.) for each gait cycle during the entire trial. The real-time implementation were programmed in MATLAB/Simulink (R2020a, MathWorks, MA, USA) together with a target machine (Speedgoat Inc., Liebefeld Switzerland). The mean dorsiflexion during swing phase of the entire trial are presented in Fig. (6).

Experimental results: Before applying FES, S01 demonstrated foot drop accompanied with little to no volitional knee flexion/extension and hip flexion/extension on the right leg. To assist gait, we formulated the MPC problem as a regulation problem with the objective of no foot drag while

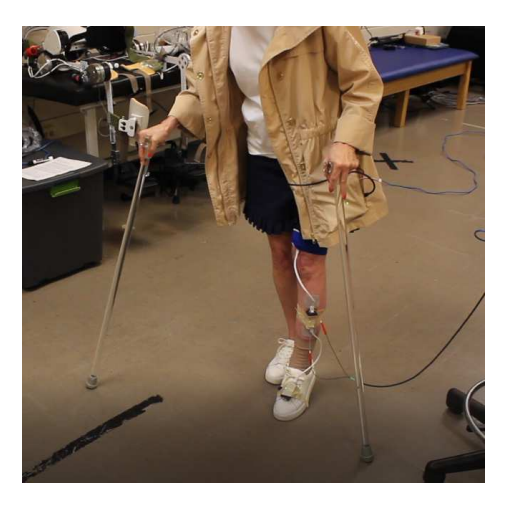


Figure 5. Walking experimental setup - During the walking task, Subject S01 performed 8 steps on an even surface and demonstrating foot clearance (> 11deg. w.r.t. the equilibrium position). The electrodes were placed on the head of the TA muscle to produce the designed FES stimulation profile for adequate foot clearance.

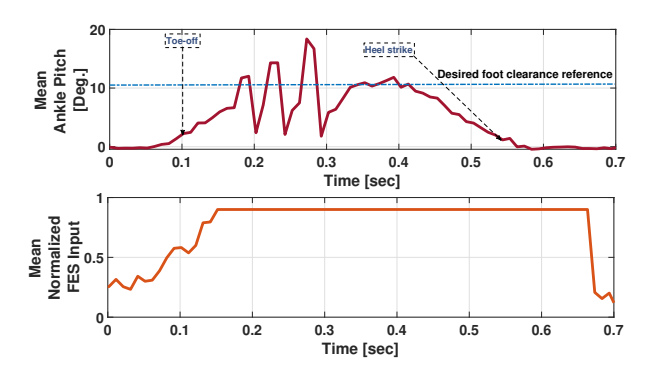


Figure 6. The plot shows the experimental results for DFC for subject with MS. The angle and stimulation profiles reflect the mean ankle dorsiflexion response for 8 steps during the swing phase under optimal FES input actuation. The spikes in the dorsiflexion angle are due to the unaccounted volitional torque of the subject. The current control is derived based on gait phase detection by IMU units. Further research will account for volitional torque under the presence of FES.

achieving adequate foot clearance (pitch, $x_1 > 12 deg$.) for each gait cycle during the swing phase. A trajectory tracking was not attempted due to inconsistent heel strike times and difficulty in timing a desired trajectory. Instead we implemented the MPC as a regulation problem. As shown in Fig. (6), adequate foot clearance was achieved during the swing phase, but oscillations in the foot pitch were also observed. We speculate the oscillations were likely due to ignoring the activation and fatigue muscle dynamics. To improve this ankle motion oscillation our future work aims to incorporate a multi-electrode placement approach that can actuate different muscles while accounting for muscle activation and fatigue dynamics.

D. Discussion & Future Work

For future work, we aim to incorporate surface electromyography and Ultrasound-based information, presented

in [20], to establish a data-driven relationship between muscle fatigue, activation dynamics, and FES stimulation parameter design enhance the closed-loop performance for DFC control. We can further use the Koopman operator framework to analyze cascaded/composite functions of state and control and analyze the preservation of nonlinear dynamics for implicit differential equations.

V. CONCLUSION

We proposed a data-driven MPC-based optimization for FES to correct foot drop. Our method is aimed to be real-time implementable without requiring a prior system identification process to determine different muscle activation and fatigue parameters. To achieve this objective, we develop a Koopman-operator based predictive controller that assists in adequate foot clearance for people with foot drop. We model FES effectuated ankle dynamics using a Koopman operator approximation, and then synthesize optimal control using MPC. We provide the recursive feasibility and asymptotic stability analysis of the closed-loop system. We have validated our design in real-time closed-loop FES experiments with seated position and walking tasks. Our findings indicate that the proposed data-driven MPC for FES can elicit the necessary ankle dorsiflexion to facilitate normal gait. The suggested FES system was used to correct the drop foot in a patient with MS.

REFERENCES

- [1] A. I. Kottink, L. J. Oostendorp, J. H. Buurke, A. V. Nene, H. J. Hermens, and M. J. IJzerman, "The orthotic effect of functional electrical stimulation on the improvement of walking in stroke patients with a dropped foot: a systematic review," *Artificial organs*, vol. 28, no. 6, pp. 577–586, 2004.
- [2] G. York and S. Chakrabarty, "A survey on foot drop and functional electrical stimulation," *International Journal of Intelligent Robotics* and Applications, vol. 3, no. 1, pp. 4–10, 2019.
- [3] M. Hayashibe, Q. Zhang, and C. Azevedo-Coste, "Dual predictive control of electrically stimulated muscle using biofeedback for drop foot correction," in 2011 IEEE/RSJ International Conference on Intelligent Robots and Systems. IEEE, 2011, pp. 1731–1736.
- [4] M. Benoussaad, K. Mombaur, and C. Azevedo-Coste, "Nonlinear model predictive control of joint ankle by electrical stimulation for drop foot correction," in 2013 IEEE/RSJ International Conference on Intelligent Robots and Systems. IEEE, 2013, pp. 983–989.
- [5] N. A. Kirsch, X. Bao, N. A. Alibeji, B. E. Dicianno, and N. Sharma, "Model-based dynamic control allocation in a hybrid neuroprosthesis," *IEEE Transactions on Neural Systems and Rehabilitation Engineering*, vol. 26, no. 1, pp. 224–232, 2017.
- [6] N. Kirsch, N. Alibeji, and N. Sharma, "Nonlinear model predictive control of functional electrical stimulation," *Control Engineering Practice*, vol. 58, pp. 319–331, 2017.
- [7] X. Bao, Z. Sheng, B. E. Dicianno, and N. Sharma, "A tube-based model predictive control method to regulate a knee joint with functional electrical stimulation and electric motor assist," *IEEE Transactions on Control Systems Technology*, vol. 29, no. 5, pp. 2180–2191, 2020.
- [8] Z. Sun, X. Bao, Q. Zhang, K. Lambeth, and N. Sharma, "A tube-based model predictive control method for joint angle tracking with functional electrical stimulation and an electric motor assist," in 2021 American Control Conference (ACC). IEEE, 2021, pp. 1390–1395.
- [9] J. L. Proctor, S. L. Brunton, and J. N. Kutz, "Generalizing koopman theory to allow for inputs and control," SIAM Journal on Applied Dynamical Systems, vol. 17, no. 1, pp. 909–930, 2018.
- [10] M. Korda and I. Mezic, "Linear predictors for nonlinear dynamical systems: Koopman operator meets model predictive control," *Automatica*, vol. 93, pp. 149–160, 2018.

- [11] M. Korda and I. Mezić, "Optimal construction of koopman eigenfunctions for prediction and control," *IEEE Transactions on Automatic Control*, vol. 65, no. 12, pp. 5114–5129, 2020.
- [12] E. Kaiser, J. N. Kutz, and S. L. Brunton, "Data-driven discovery of koopman eigenfunctions for control," arXiv preprint arXiv:1707.01146, 2017.
- [13] N. Sharma, C. M. Gregory, M. Johnson, and W. E. Dixon, "Closed-loop neural network-based nmes control for human limb tracking," *IEEE Transactions on Control Systems Technology*, vol. 20, no. 3, pp. 712–725, 2011.
- [14] G. Mamakoukas, M. Castano, X. Tan, and T. Murphey, "Local koop-man operators for data-driven control of robotic systems," in *Robotics: science and systems*, 2019.
- [15] M. Budisic, R. Mohr, and I. Mezic, "Applied koopmanism," Chaos: An Interdisciplinary Journal of Nonlinear Science, vol. 22, no. 4, p. 047510, 2012.
- [16] K.-S. Park, J.-B. Park, Y.-H. Choi, T.-S. Yoon, and G. Chen, "Generalized predictive control of discrete-time chaotic systems," *International* journal of bifurcation and chaos, vol. 8, no. 07, pp. 1591–1597, 1998.
- [17] L. Burner and N. Sharma, "A wearable sensing system to estimate lower limb state for drop foot correction," *Highlighting Undergraduate Research at the University of Pittsburgh Swanson School of Engineering*, p. 16, 2018.
- [18] P. Muller, T. Steel, and T. Schauer, "Experimental evaluation of a novel inertial sensor based realtime gait phase detection algorithm," in *Proceedings of the Technically Assisted Rehabilitation Conference*, 2015.
- [19] T. Seel, C. Werner, J. Raisch, and T. Schauer, "Iterative learning control of a drop foot neuroprosthesis generating physiological foot motion in paretic gait by automatic feedback control," *Control Engineering Practice*, vol. 48, pp. 87–97, 2016.
- [20] Q. Zhang, A. Iyer, Z. Sun, K. Kim, and N. Sharma, "A dual-modal approach using electromyography and sonomyography improves prediction of dynamic ankle movement: A case study," *IEEE Transactions* on Neural Systems and Rehabilitation Engineering, vol. 29, pp. 1944– 1954, 2021.